Optical properties of GaSe and GaS_xSe_{1-x} mixed crystals

M. Schlüter,* J. Camassel,† S. Kohn, J. P. Voitchovsky,‡ Y. R. Shen, and Marvin L. Cohen§
Department of Physics, University of California and Inorganic Materials Research Division, Lawrence Berkeley Laboratory, Berkeley, California 94720
(Received 11 September 1975)

Reflectivity and wavelength-modulated reflectivity measurements on GaSe and GaS_xSe_{1-x} mixed crystals are presented for energies ranging from 3 to 6 eV. Additional electroreflectance measurements are used to investigate the excitonic character of the structure at 3.4 eV in GaSe. The results are discussed on the basis of a new pseudopotential band-structure calculation for GaSe. The prominent spectral structures of GaSe are identified in terms of location in $\vec{k}$ space and atomic character of the states involved in the transitions. The main structures in the optical-response function of GaSe are found to result from excitations of the Ga–Ga bond and from atomiclike transitions between nonbonding Se p and s states. These main transitions are located in $\vec{k}$ space close to symmetry determined "special $\vec{k}$ points." The observed mixed-crystal spectra can be decomposed into three classes of transitions which exhibit zero, intermediate, and strong energy shifts with anion substitution. Theoretically, the three classes of transitions are found to take place between states with zero or little, intermediate, and large charge concentrations on the anion sites. Thus, the characteristic energy shifts, observed experimentally can directly be related to atomic spectral properties of sulphur and selenium.

I. INTRODUCTION

The semiconducting III-VI compounds GaSe and GaS crystallize in layer structures. The arrangement of atoms within one layer is identical in both compounds. Three different types of regular stackings of the layers have been described in the literature, as β, ϵ, and γ modifications, respectively.[1,2] Monocrystals of GaSe grown by the Bridgman technique normally contain a mixture of ϵ and γ modifications, whereas the stacking of layers in GaS monocrystals is invariably of the β-type.[3,4]

GaSe and GaS form a continuous series of mixed crystals GaS_xSe_{1-x}.[5,6] For $0.6 \leq x \leq 1$, the β modification predominates and the ϵ and γ modifications are found to $0 \leq x \leq 0.1$. In the intermediate region all three types of stacking occur.[5] Despite the fact that these crystals clearly exhibit two-dimensional structure and consequently have highly anisotropic mechanical properties, it has been argued that not all electronic states reflect this anisotropy. In particular, recent three-dimensional band calculations[7,8] as well as measurements of optical properties and of electronic transport properties have indicated that GaSe has nearly isotropic electronic states at the forbidden gap.[9] However, further away in energy from the fundamental gap more anisotropic states are predicted by theory.[8] Until now no attempt has been made to use the band-structure calculations to analyze the electronic transitions at higher energies. The first part of this paper therefore concentrates on these questions. The main reflectivity structure of GaSe observed in the range 3 to 6 eV will be assigned to particular transitions and a new, slightly modified band-structure calculation will be presented.

Studies of the phonon modes of mixed GaS_xSe_{1-x} crystals via nonresonant Raman-scattering experiments[10,11] have shown that besides continuous energy shifts of some of these modes with composition, other modes exhibit discontinuities in their energy shifts or appear only in the intermediate region of composition for $x \neq 0$ or 1. These discontinuities were associated with "two-mode" behavior, local modes, or with stacking effects.[11] The latter give rise to a drop off in the intensity of the 135-cm^{-1} Raman mode around $x = 0.6$ which is the consequence of a change from $\epsilon - \gamma$ stacking to β stacking of the layers in which this mode becomes Raman inactive. Furthermore, initial studies[6] of the optical absorption of GaS_xSe_{1-x} at the fundamental edge have given additional experimental indication of structural disorder in these compounds. For $x \sim 0.4$, a step of 50 meV was found in the energy position of both direct and indirect gap transitions. This step was attributed to the difference in energy between the absorption onsets in the γ, ϵ, and β polytypes. Another interesting effect aside from the above-mentioned discontinuities found both in absorption[6,12,13] and luminescence experiments[14,15] is the linearity of the energy shifts of the gaps with composition x. No measurable nonlinearity has been observed and the shifts between GaSe and GaS are $\Delta \simeq 0.8$ eV for the direct gap and $\Delta \simeq 0.4$ eV for the indirect gap.

It will be shown that similar properties are also observed in the optical transitions in the range between 3 and 6 eV. A specific energy shift Δ is associated with each main transition observed in the complete GaS_xSe_{1-x} alloy system. Within experimental accuracy (± 0.1 eV), only three dif-

ferent values of Δ are found for the observed structures. Thus all transitions can be grouped into three classes, each of which is characterized by the atomic character of the wave functions of initial and final states associated with the transition. The observed spectra of GaS_xSe_{1-x} mixed crystals can thus be understood using a model of distinct and differently localized atomiclike transitions.

The remainder of this paper is organized as follows. In Sec. II the experimental procedure is described. Section III contains a detailed discussion of the reflectivity and modulated reflectivity of GaSe between 3 and 6 eV and their interpretation on the basis of a new band-structure calculation. In Sec. IV the observed spectra of GaS_xSe_{1-x} mixed crystals are examined and interpreted on the basis of the calculated electronic structure of GaSe.

II. EXPERIMENTAL PROCEDURE

The experimental apparatus and wavelength modulation spectrometer used in this experiment have been described elsewhere.[16] The system is operated in a configuration that measures $R(\lambda)$ and $dR/Rd\lambda$ simultaneously. A double beam method is used to cancel the background contribution to the derivative signal. In order to compare with theory the spectra are digitized and converted into $R(E)$ and dR/RdE. All the samples used in this experiment were cleaved in the plane of the layers from large single-crystal ingots. The single crystals were grown by the Bridgman technique in sealed quartz ampoules. The starting materials consisted of an admixture of pure (99.9999) polycrystalline GaSe and GaS intimately mixed in the ampoule before growth. Although the melting temperatures of GaSe and GaS are very similar (~1000 °C), it should be noted that the growth of the mixed crystals is considerably more difficult than that at the pure compounds. Except for the top end of the ingots, no noticeable variations of composition have been found for crystals grown under appropriate conditions. Furthermore, the formation of voids was prevented by growing the crystals under a pressure of several Torr of pure argon.

The compositions were measured by an ionic microprobe technique and found to have the following values: $x = 0.10$; 0.22; 0.31; 0.40; 0.47; 0.51; 0.57; 0.66; 0.72; 0.76; 0.91. The samples are homogeneous within 1%. Unless specified, all data were taken at 5 °K with the samples kept on top of a liquid-helium bath. The measurements are taken with unpolarized light incident approximately parallel to the c axis.

III. BAND STRUCTURE AND REFLECTIVITY OF GaSe

Even though recent three-dimensional band-structure calculations of[7,8] GaSe were able to explain most of the chemical bonding properties,[8] the optical properties in the vicinity of the fundamental gap[17] and the electrical properties,[9] their accuracy for energies further away from the fundamental gap remained somewhat unclear. Preliminary joint density-of-states calculations[8] were crude and could not be matched very well to existing reflectivity data.[18] More recent ultraviolet-photoemission (UPS) data[19] also showed some disagreement with a density of states histogram obtained from the band structure of Ref. 8. This disagreement in energy for electronic states further away from the optical gap resulted from the fact that detailed experimental data at higher energies had not been available at the time the band structure[8] calculations were done. The advent of new high-resolution reflectivity data,[20,21] UPS,[19] and x-ray photoemission (XPS) data[22] has provided enough experimental information to reexamine the band structure of GaSe over a large energy range.

A first, semiquantitative attempt is presented in this paper. The new modified band structure does not account quantitatively for all observed experimental data, but it is of sufficient precision to be used along with physical arguments to explain the measurements and to understand the nature of many observed effects. To modify the existing band structure[8] of GaSe some crystal-structure parameters are changed before attempting to readjust the pseudopotential form factors. As already argued in Refs. 8 and 19 the interatomic distances, in particular the Ga–Ga distance in the middle of each layer are very inaccurately determined experimentally. The calculation in Ref. 8 was based on a Ga–Ga spacing at 2.39 Å which corresponds to the upper limit allowed by experiment.[2] As stated before[19] this distance is about 5% smaller than twice the covalent radius of Ga,[23] $r = 1.26$ Å, and therefore somewhat doubtful.

A simple and obvious modification of the band structure is thus obtained by using a Ga–Ga spacing of twice the covalent radius of Ga (2.52 Å) and by retaining the pseudopotential form factors of Ref. 8. The resulting band structure (the lowest four Se s bands are not shown) is presented in Fig. 1. The calculations were performed at a somewhat lower stage of convergence than in Ref. 8. Plane waves up to a kinetic energy of 3.0 Ry were included directly together with plane waves up to 6.0 Ry which were included by second-order perturbation theory. The potentials used are those given in Ref. 8. As expected, an increase in the Ga–Ga bond length decreases the gap between bands 5, 6 and 7, 8 (the first two groups of bands in Fig. 1). These bands have predominantly bonding and antibonding Ga s char-

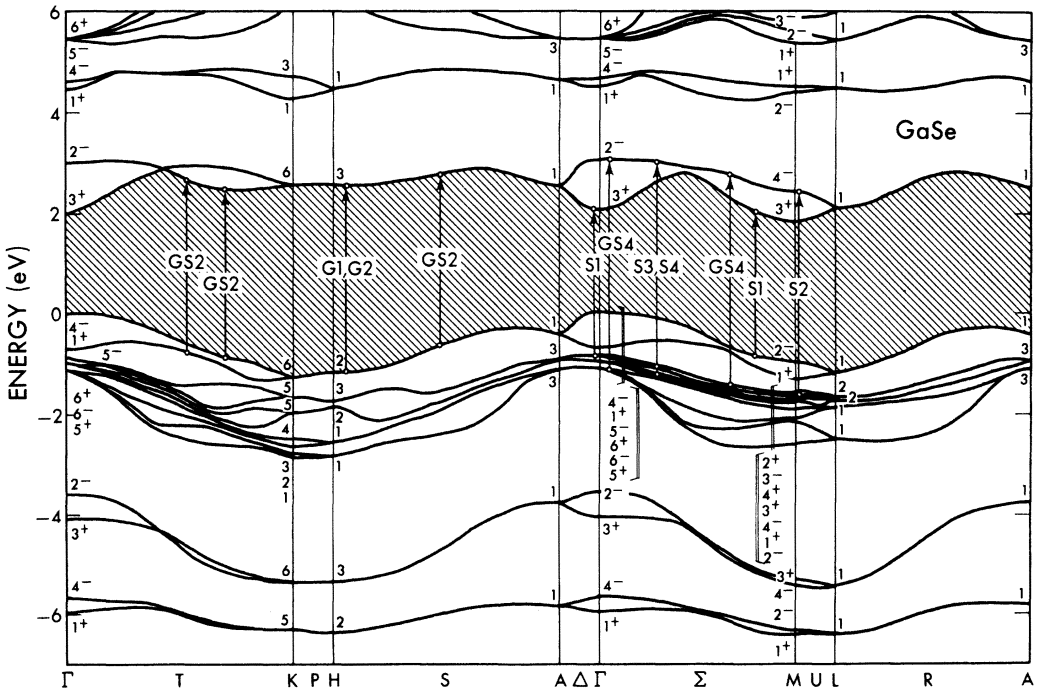

FIG. 1. Band structure of GaSe along the principal high-symmetry lines of the hexagonal Brillouin zone. Lowest four Se *s* bands are not shown in the figure. Energy levels are labeled according to Herring's notation of the space group D_{6h}^4. Some transitions resulting in prominent structure in the reflectivity spectrum are indicated.

acter.[8] This is in good agreement with XPS data.[22] The same deformation also raises the topmost valence band (18) and its partner (17), both of which show considerable bonding charge between the two Ga atoms. In fact, the two bands are now raised completely above the Ga-Se bands (10-16) in contrast to the band structure of Ref. 8. This increases the width of the group of bands 10 to 18 which is also in agreement with XPS data. All symmetries and selection rules for direct and indirect gaps remain unaltered with small changes in their respective energies. The conduction band structure remains essentially unchanged exhibiting a large 1.5-eV gap between the first and second pair of bands. Evidence for the existence of this gap has been obtained from recent core-to-conduction-band reflectivity measurements using synchrotron radiation.[21]

In Fig. 2 the calculated and measured reflectivity for energies between 3 and 6 eV are displayed. To calculate the reflectivity, first the imaginary part of the dielectric function $\epsilon_2(\omega)$ has been evaluated up to an energy of about 8 eV; then the real part $\epsilon_1(\omega)$ is obtained by Kramers-Kronig transformation. Since some important structure in the dielectric function exists beyond 8 eV,[21] the calculated $\epsilon_1(\omega)$ and hence the reflectivity are too low in magnitude; the position of structures below 6 eV, however, should not be affected by the low cutoff. The calculated reflectivity curve had to be shifted by 0.4 eV to higher energies to achieve satisfactory agreement with experiment. Since all important transitions below 5.5 eV terminate at the first conduction band pair (bands 19, 20), the shift of the reflectivity curve can easily be obtained by rigidly shifting upwards the main portions of bands 19 and 20. In view of this feature, assignments of structure in the reflectivity curve can safely be made on the basis of the present band structure and no attempt was made to quantitatively readjust pseudopotential form factors.

Although the experiment was performed in the $\vec{E} \perp \vec{c}$ geometry a small finite angle of incidence (~5°) and the finite aperture of the light beam (~5°) allow the presence of an $\vec{E} \parallel \vec{c}$ component. Due to this small $\vec{E} \parallel \vec{c}$ component which is combined with a strong matrix element anisotropy[17] the experimental spectra are most conveniently compared to an *unpolarized* calculated spectrum. The precise position of structure in the measured and calculated reflectivity is obtained from the respective derivative spectra (Fig. 3). Their energy values together with the band-structure assignment are given in Table I. The main transitions are also indicated directly in the band structure diagram (Fig. 1). The labeling has been chosen to indicate whether cation gallium (*G*) or anion selenium (*S*) or both atomic characters are present in the initial and final states defining the

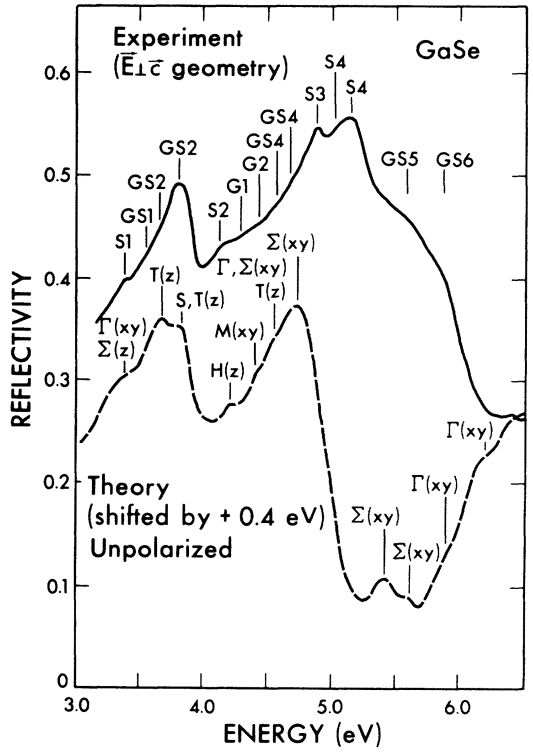

FIG. 2. Experimental (full line) and calculated (broken line) reflectivity of GaSe. Theoretical curve has been shifted by 0.4 eV to higher energies as described in the text. Structures in the experimental spectrum are labeled according to Table I. Corresponding labeling of the theoretical curve refers to $\vec{k}$-space location and polarization dependence of the transitions involved.

transition. Typical transitions will be discussed in these terms later in Sec. IV. The first main peak ($GS2$) around 3.8 eV (E_1 in the notation of Ref. 18), originates from transitions between the uppermost valence-band pair (17, 18) and the first conduction band pair (19, 20) around T and S and corresponds to an excitation of the Ga–Ga bond and of nonbonding Se p_z to s transitions. The second main peak ($S3$, $S4$) around 5.0 eV (E_3 in the notation of Ref. 18) originates mainly from transitions starting from the lower lying Ga–Se bands (14, 16) around Σ and involves exclusively Se p_{xy} to s transitions. As indicated in Fig. 2 and Table I the two main peaks are expected to show opposite polarization dependence.

It is of interest to note that these two groups of transitions which roughly determine the lower part ($E<6$ eV) of the reflectivity spectrum take place at locations in the hexagonal Brillouin zone which are close to "special $\vec{k}$ points" as defined by Baldereschi,[24] and by Chadi and Cohen.[25] These authors have developed a scheme for evaluating sums over wave vector in the Brillouin zone of a periodic function. They have found that by choosing special points in $\vec{k}$ space, rapid convergence of the sum can be achieved. Physically this means that from these special $\vec{k}$ points which are solely determined by the crystal-point and translational symmetry, an optimum zero-order approximation for various quantities such as electronic charge densities can be obtained. Moreover, in the present reflectivity spectrum the $GS2$ peak at 3.8 eV could be adequately approximated by evaluating the band structure just at one special $\vec{k}$ point $\vec{k}_1 = (0.19, 0.19, 0.25)$ and the $S3$, $S4$ peak around 5.0 eV by using another special $\vec{k}$ point $\vec{k}_2 = (0.3, 0, 0.25)$. This seems to indicate that the special point scheme might also be applicable in evaluating the sum over wave vector needed for dielectric function calculations. Similar results are reported for Ge by Chelikowsky and Cohen.[26] It should be emphasized, however, that important structure in the dielectric function of GaSe appears at energies higher than 6 eV.[21] No analysis and structure assignment has yet been made in this energy range and the validity of the special point approximation for higher energies is yet to be investigated.

One particular transition ($S1$) in the rising shoulder of the first peak ($GS2$) in the reflectivity

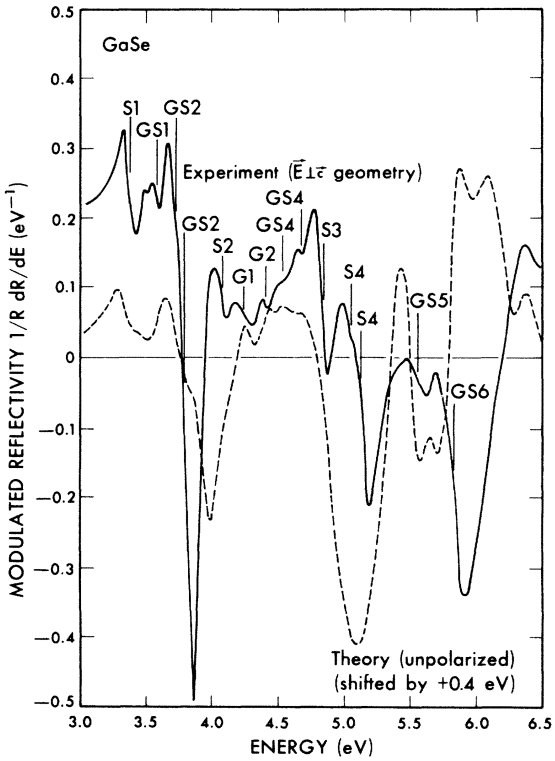

FIG. 3. First energy derivative spectrum obtained from the measured (full line) and theoretical (broken line) reflectivity of Fig. 2. Shift of the theoretical curve and the labeling is as in Fig. 2.

TABLE I. Listing of experimental (5 °K) energies for the main structures in the reflectivity spectrum of GaSe. The theoretical assignment of $\vec{k}$-space location, polarization dependence, and band numbers of the involved transitions are also listed. The experimental (5 °K) energies of corresponding structures in GaS are given in the last column.

	GaSe			GaS
	Experiment		Theory	Correspondence
Label (this work)	Energy 5 °K	Label (Ref. 18)	Assignment	Energy 5 °K
*S*1 (excit.)	3.37			4.55
*S*1	3.40		$\Gamma(xy)$ 16 – 19	4.61
*GS*1	3.58		$\Sigma(z)$ 18 – 19	
	3.70		$T(z)$ 18 – 19	
*GS*2	3.80	E_1	$T, S(z)$ 17 – 19	4.03
*GS*3	•••			4.20
*S*2	4.07	E_2	$M(z,y)$ 15 – 20	4.82
*G*1	4.28		$H(z)$ 18 – 19	4.30
*G*2	4.41			4.42
*GS*4	4.54 4.67		$\Sigma(xy)$ 16 – 20 $\Gamma(xy)$ 16 – 20 $T(z)$ 17 – 20	4.82
*S*3	4.86	E_3	$\Sigma(xy)$ 16 – 20	5.57
*G*3	5.03		•••	5.03
*S*4	5.13	E_3'	$\Sigma(xy)$ 14 – 20	5.78
*G*4	•••			5.23
*GS*5	5.56	E_4	$\Sigma(x,y)$ 18 – 20	5.90
*GS*6	5.83	E_4'		6.20

curve which is of particular interest is discussed below. According to the band-structure calculation the structure observed around 3.4 eV at 5 °K is identified with the transition $\Gamma_5^- - \Gamma_3^+$. This transition which involves the 15th and 16th (degenerate at Γ) valence band and the first conduction band (19) is of predominantly anion (Se) character, i.e., its initial state contains mostly Se p_x, p_y character and its final state shows appreciable Se *s* admixture. This point shall be discussed in more detail and illustrated by charge-density contours in Sec. IV together with interpretation of results on GaS_xSe_{1-x} mixed crystals.

Since its first observation in absorption by Subashiev *et al.*[27] in 1971, the *S*1 transition has been extensively studied and successively assigned to (i) a saddle-point exciton,[28,29] to (ii) a M_1 critical point (c.p.),[30,31] or to (iii) an excitonic transition at a M_0 c.p.[32,33] To emphasize the excitonic character of the transition in Fig. 4 the comparison is made between (a) the wavelength modulated reflectivity at 300 °K, (b) a room-temperature electroreflectance (ER) spectrum, (c) the reflectivity at room temperature, and (d) the reflectivity at 5 °K.

The ER measurements are obtained by the electrolytic method, following the prescriptions of Ref. 30 and lead to results similar to those of Ref. 30. The striking feature of the ER spectrum is that the most important response is *not* obtained at the main reflectivity structure (*GS*2 at 3.68 eV at 300 °K) but rather on the small shoulder (*S*1) seen at 3.21 eV at 300 °K. The larger electro-optic enhancement clearly confirms the excitonic character of this structure. The nature of the corresponding critical point and the binding energy of the exciton are subject to discussion.[29,33] The binding energies reported so far range from 318 meV (for a[28] M_1 c.p.) to 9 meV (for a[33] M_0 c.p.) and depend strongly on the theoretical model used to interpret the data. In the present case for the first time a direct measurement of the exciton binding energy can be given.

On high quality crystal samples the reflectivity peak could be resolved into two components at low

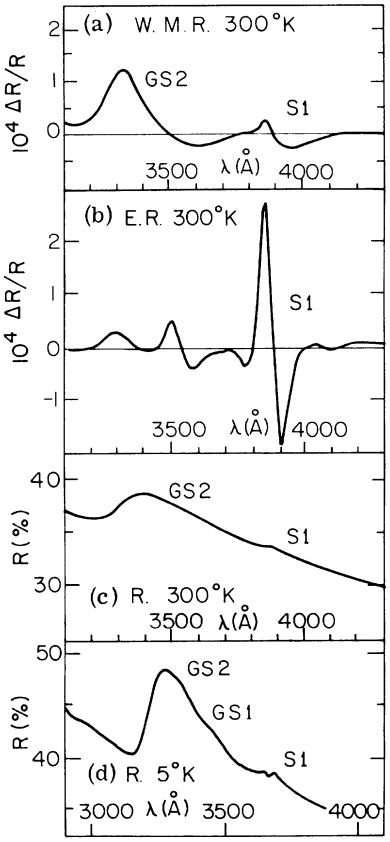

FIG. 4. Several room- and low-temperature spectra of the *S*1 structure in GaSe around 3.4 eV. (a) Room-temperature wavelength modulated reflectivity spectrum, (b) differential electroreflectance spectrum at room temperature, (c) room-temperature reflectivity spectrum, (d) reflectivity spectrum at 5 °K. Note the well-resolved doublet structure.

temperatures [Fig. 4(d)]. They are attributed to the excitonic ground state and the corresponding continuum transitions. The observation of an $n=2$ excited exciton state can be ruled out on the basis of oscillator strength and lifetime arguments. The two well-resolved structures are found at 3.37 and 3.40 eV at 5 °K, from which an exciton bonding energy of $E_B = 30 \pm 5$ meV is deduced. Though the two-peak structure can clearly be observed, it is too limited in amplitude to allow an accurate line-shape analysis. However, with the binding energy directly measured, different theoretical models can now be critically analyzed in connection with information obtained from the band structure and from other independent experiments.[34] Thus the following four excitonic models will be analyzed: (i) a three-dimensional isotropic exciton at a[35] M_0 c.p.; (ii) a strictly two-dimensional exciton[36]; (iii) a three-dimensional hyperbolic exciton[37]; (iv) a three-dimensional anisotropic exciton at a[38] M_0 c.p. Using the accepted values of $\epsilon_{0\parallel} = 7.6$ and $\epsilon_{0\perp} = 10.2$ for the static dielectric constant[39] and a binding energy of 30 meV, the band masses compiled in Table II are obtained for the various models.

The isotropic M_0-type exciton model leads to a reduced mass of $\mu = 0.17$ which at the same time represents the lower limit for the mass $\mu_\parallel$ along the c axis. Taking into consideration the anisotropic conduction-band masses of Ref. 34, ($m_{c\parallel} = 0.3$ and $m_{c\perp} = 0.17$) which have been obtained independently by magneto-optical and transport measurements, the isotropic case (i) can be dismissed since it would require a very strong anisotropy of opposite sign for the valence band mass. The two-dimensional and the hyperbolic exciton models both result in a transverse mass of $\mu_\perp = 0.06$. These two cases can be dismissed for similar reasons as case (i). The band structure of Fig. 1 indicates that an anisotropic M_0-type c.p. is most likely to be involved in the $S1$ transition. While the isotropic limit for the longitudinal mass is $\mu_\parallel = 0.17$, the anisotropic limit is $\mu_\parallel = 0.3$ determined from the conduction-band mass, assuming the valence-band masses to be large. (These limits exclude recently proposed masses, obtained by analyzing ER data.[33]) If the valence-band masses are much heavier than the conduction-band masses, which can safely be inferred from the band structure in Fig. 1,[40] the reduced masses are simply given by $\mu_\parallel \approx m_{c\parallel} = 0.3$ and $\mu_\perp \approx m_{c\perp} = 0.17$. The values result in an anisotropy parameter

$$\alpha = \mu_\perp \epsilon_\perp / \mu_\parallel \epsilon_\parallel = 0.76 ,$$

which leads to an exciton binding energy of $E_B^{\text{calc}} = 33$ meV, in excellent agreement with the measured value. In conclusion a three-dimensional anisotropic M_0 c.p. exciton with 30 meV binding energy seems most likely to be the nature of the 3.4-eV structure in the reflectivity spectrum of GaSe. The measured binding energy is in excellent accord with (a) independently determined conduction-band masses and (b) theoretical band-structure calculations.

TABLE II. Reduced effective masses of bands 16 and 19 at the Γ point in GaSe as obtained from various electroabsorption and electroreflectance measurements and from several theoretical models invoked to explain the structure $S1$ around 3.4 eV in GaSe.

Technique or theoretical model	Reference	$\mu_\perp$	$\mu_\parallel$
EA (ionization field)	a	0.089	
ER (ionization field)	a		0.16
ER (period of oscillations)	a	0.014-0.09	0.09
M_0 c. p. (isotropic 3-D exc.)	b	0.17	0.17
M_0 c. p. (2-D exc.)	b	0.06	∞
M_1 c. p. (hyp. exc.)	b	0.06	∞
M_0 c. p. (anisotropic 3-D exc.)	c	~0.17	~0.3

[a]After Ref. 33, EA: electroabsorption, ER: electroreflectance.

[b]This work, $E_B = 30$ meV.

[c]This work, $E_B = 30$ meV, $m_{c\parallel} = 0.3\, m_0$, $m_{c\perp} = 0.17\, m_0$ after Ref. 9.

IV. REFLECTIVITY OF GaS_xSe_{1-x} MIXED CRYSTALS

In this section, detailed reflectivity and wavelength modulated reflectivity spectra of the complete GaS_xSe_{1-x} mixed-crystal series are presented. In the range of interband transitions, these data represent the first systematic measurements of this kind performed on this system. Previous results[20,41,42] did not establish a clear picture of the shift of interband transitions between GaSe and GaS. In the present work the spectral changes observed in the mixed-crystal series are interpreted on the basis of the theoretical understanding of the GaSe spectrum presented in Sec. III.

Both reflectivity and wavelength modulated reflectivity have been measured at about 5 °K for a series of ten mixed crystals. The composition x of GaS_xSe_{1-x} varies gradually by steps of about $\frac{1}{10}$ from 0 to 1. The exact values of x determined by a microprobe technique are given in Sec. II. In Fig. 5 an illustration of the general variation of the reflectivity spectrum is given. Despite an increased broadening of the spectra for intermediate compositions, probably resulting from structural disorder and despite a weakening of some spectral structures, most of the assigned structures of GaSe (Table I) can be followed through the series to GaS (see Table I, last column).

The following general trends can be noted from Fig. 5 and Table I: (i) The main structures shift

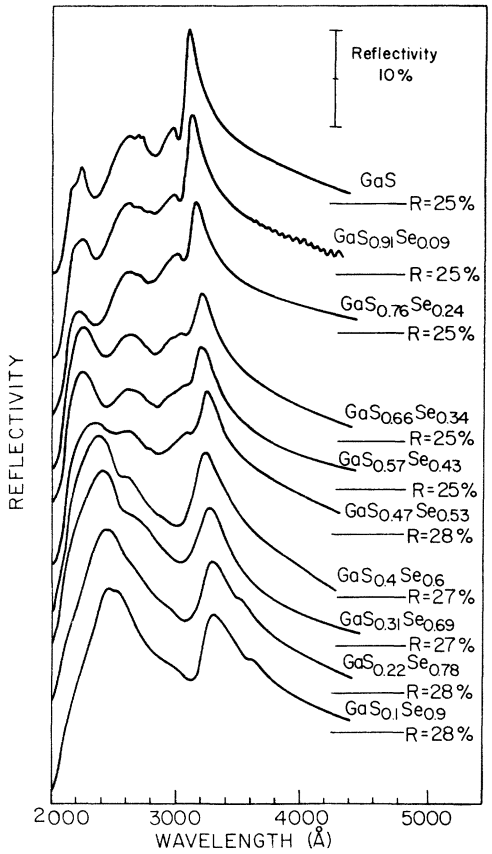

FIG. 5. Reflectivity spectra of ten GaS_xSe_{1-x} mixed crystals measured at 5 °K between 3 and 6 eV.

to higher energies for increasing sulphur concentration x. (ii) The low energy peak $GS1$, $GS2$ (at 3.8 eV in GaSe) narrows considerably with increasing x resulting in a very sharp dominating structure in GaS. This will be discussed in more detail later. (iii) The characteristic two-peak structure of GaSe gradually transforms into a more complicated spectrum in GaS.

Detailed analysis of the spectral changes as a function of x reveals linear shifts for almost all important structures. Moreover, according to their shifts (Δ), these structures, including direct and indirect gap at about 2.0 eV,[6] can be grouped into three different classes with zero ($\Delta \approx 0$), intermediate ($\Delta \approx 320$–400 meV) and strong ($\Delta \approx 780$ meV) shifts, respectively. They will be discussed separately below. For each class one representative transition of GaSe is investigated theoretically in detail. Charge-density contour maps are used to illustrate the corresponding atomic character of initial and final states. The various energy shifts Δ may in turn be inferred from the atomic character of the wave functions of initial and final states. In addition, an optical transition function $\vec{F}(\vec{r}) = \psi_i(\vec{r})\vec{p}\,\psi_f(\vec{r})$, where $\vec{p}$ is the momentum operator, has been defined. The integral $\vec{M}_{if} = \int \vec{F}(\vec{r})\,d\vec{r}$ of this function represents the optical dipole matrix element and describes the strength and polarization of the transition. In examining transition functions $\vec{F}(\vec{r})$ which lead to nonzero dipole matrix elements $\vec{M}_{if}$, additional information about *real-space* localization of optical transitions can be obtained. This information may be used to discern between atomiclike (intraionic), charge-transfer-like (interionic) or bondlike (bonding-antibonding) transitions. These are described in Secs. IV A–C.

A. Transitions with strong cation (Ga) character and zero energy shift ($\Delta \approx 0$ meV)

Four main structures of Table I labeled $G1$ to $G4$ (G strands for predominant gallium character in the corresponding wave functions) belong to the $\Delta = 0$ class. Their energies which are displayed in Fig. 6 as a function of composition x show no overall shift if sulphur is substituted for selenium. Experimentally $G1$ and $G2$ can easily be followed through the entire composition range, whereas $G3$ and $G4$ are only resolved in crystals with higher sulphur concentration. For low values of x, $G3$ and $G4$ merge with the strong S_3, S_4 structure which dominates the spectrum in this energy range and cannot be resolved. In GaSe the structures $G1$, $G2$ are assigned to transitions between the topmost valence band and the bottom conduction band near the point H in the hexagonal Brillouin zone (see Fig. 3). The two-fold degeneracy of the valence band at H (see Fig. 3) is lifted by the inclusion of spin-orbit interaction. The re-

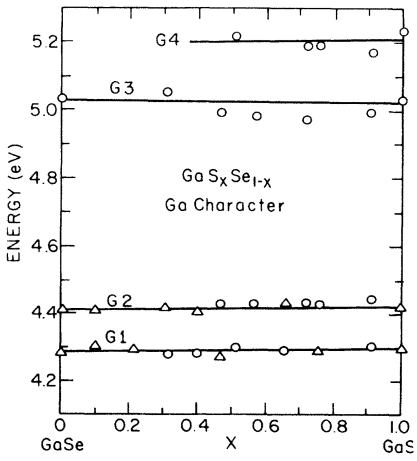

FIG. 6. Energy diagram of structures observed in the GaS_xSe_{1-x} mixed-crystal reflectivity which exhibit $\Delta \approx 0$ energy shift. Structures are labeled $G1$ to $G4$ indicating the predominant anion (gallium) character in the wave functions of initial and final states. Well-resolved structures are indicated by circles, weak structures by triangles.

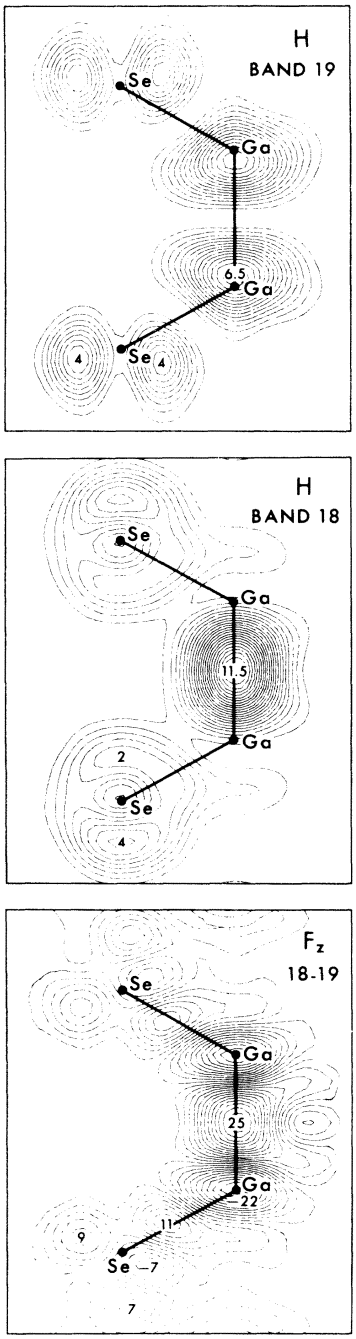

FIG. 7. Charge-density contour plots of valence-band state (middle figure) and conduction-band state (top figure) at point H in the Brillouin zone of GaSe. Transition between these states which gives rise to the $G1$ ($G2$) structures indicated in Figs. 1 and 2 and in Table I is chosen as representative for gallium (G)-like transitions of Fig. 6. The transition function F_z (bottom figure) which indicates the real-space location (around the gallium atoms) of the transition is defined in the text. All contour plots are displayed in a (110) plane extending over one layer of GaSe. Charge-density contours are given in units of electrons per (two-layer) unit cell; the transition function contours are given in atomic units.

sulting splitting which according to an analysis of the wave functions should result from Ga p levels is most likely to be responsible for the double structure $G1$, $G2$. This assignment is strongly supported by the observation of a constant splitting of 0.12 eV between $G1$ and $G2$ throughout the entire alloy series. Moreover, the observed value of 0.12 eV agrees well with the atomic Ga $3p$ spin-orbit splitting of about 0.09 eV.[43]

In Fig. 7 charge-density contour plots from both initial and final states of the $G1$, $G2$ transitions in GaSe are presented together with the connecting transition function F_z. (The transition is allowed for polarization $\vec{E} \parallel \vec{c}$.) The plots are given in a (110) plane extending over one layer (half the unit cell). The charge-density contours are given in units of one electron per unit cell. The transition function is given in atomic units. As seen from the charge-density contours, charge in both states is concentrated in the vicinity of the Ga atoms and only a little charge sits around the anions. This obviously explains the negligible shift of the transition energy if sulphur is substituted for selenium. The charge distribution exhibits the bonding (band 18) and antibonding (band 19) character of the Ga–Ga bond. This bond can be excited optically as illustrated by the transition function F_z (bottom Fig. 7).

The transitions $G1$ to $G4$ thus represent the particular case of pure cation transitions whose energy is not or slightly affected by anion substitution. The existence of these transitions is believed to be caused by the particular GaSe, GaS crystal structure in which like-atom bonds (cation-cation) exist. Conversely, no zero-shift transitions are found in the zinc-blende mixed-crystal systems[44,45] which most likely have alternating anion-cation arrangements.

B. Transitions with mixed anion (S, Se)-cation (Ga) character and intermediate energy shifts ($\Delta = 320$ to 400 meV)

In Fig. 8 the energies of several transitions ($GS1$ to $GS6$) are displayed as a function of concentration x. The measured energy shifts can be fitted linearly with slopes varying between 320 and 400 meV. The structure labeled $GS1$ which corresponds to a small shoulder in the reflectivity cannot be observed for $x > 0.3$, not even in the wavelength modulated spectrum. $GS2$ corresponds to the main structure found in the reflectivity of GaSe at 3.8 eV. The shift of this structure is found to be linear with concentration for $x > 0.2$. For $x > 0.3$ the two structures $GS2$ and $GS3$ overlap resulting in a broad peak with little resolved fine structure. The possibility of connecting $GS1$ and $GS3$ by a discontinuity of 200 meV at about $x = 0.3$ similar to the observed 50-meV step of direct and indirect gap[6] due to changes

in the stacking sequence cannot be ruled out in spite of the large energy difference. As seen in Fig. 5 the shape of the *GS*2, *GS*3 structures changes drastically between GaSe and GaS. The peaks narrow considerably with increasing sulphur concentration and become the predominant features of the reflectivity spectrum for $x > 0.5$. The splitting between *GS*2 and *GS*3 which is not resolved for $x < 0.3$ has a value of 0.17 eV in GaS.

According to the assignment in GaSe the transitions take place between the topmost valence bands and the lowest conduction bands along the line T, S and their connecting line in $\vec{k}$ space (see Fig. 1 and Table I). Interlayer interaction is not likely to cause the *GS*2, *GS*3 splitting because of the very different oscillator strength of the transitions in GaS. In fact the line shape of the strong *GS*2 peak in GaS is reminiscent of the asymmetric singularity associated with a two-dimensional M_0 c.p. excitonic transition.[46,47] Indeed, a comparative inspection of the GaSe band structure (Fig. 1) lends some support to the existence of a two-dimensional M_0 c.p. for GaS in the T, S region of $\vec{k}$ space.

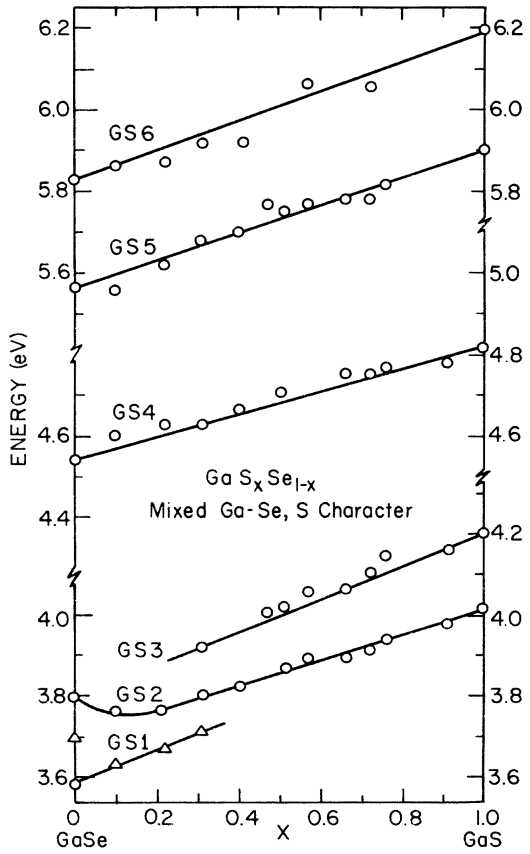

FIG. 8. Energy diagram of reflectivity structures, labeled *GS*1 to *GS*6, exhibiting intermediate ($\Delta \approx 400$ meV) energy shift. Labeling refers to mixed cation (Ga) and anion (Se, S) character of the involved wave functions.

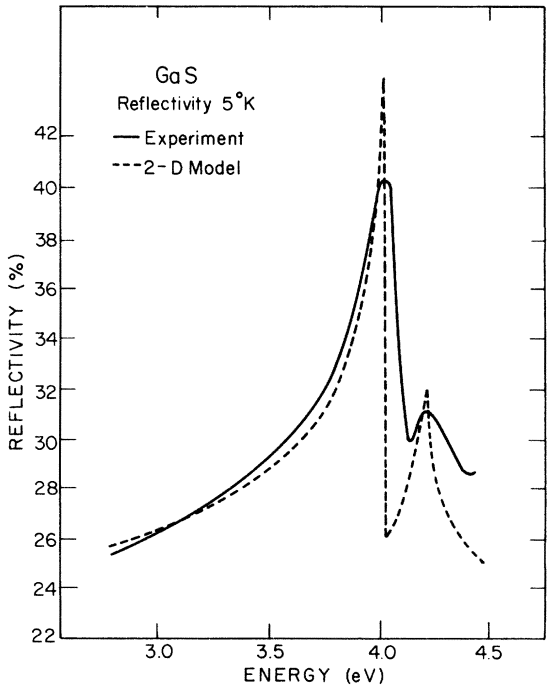

FIG. 9. Experimental (full line) and calculated model (broken line) reflectivity of structures around 4.0 eV in GaS. A two-dimensional M_0 c.p. exciton model and its associated continuum transition are used in the model reflectivity as explained in the text.

On the other hand, *no* excitonic character would be needed to explain the *GS*2 line shape if one assumes a nearly degenerate pair of two-dimensional $M_0 + M_1$ c.p.'s. The observed strong temperature dependence of the *GS*2 peak is compatible with both models. The likelihood of the observation of a two-dimensional M_0 c.p. exciton followed by the c.p. band edge for the *GS*2, *GS*3 structures in GaS is illustrated in Fig. 9. Since the real part of the refractive index dominates the imaginary part by a factor of about 10 in this energy range,[32] the reflectivity can be calculated from the functional behavior of $\epsilon_1(\omega)$ alone. The fit of the reflectivity in Fig. 9 is obtained with a background dielectric constant of $\epsilon_1 = 7$, a band-edge transition energy of $E_0 = 4.195$, and an exciton binding energy of 170 meV. No additional lifetime broadening is included and an oscillator strength of unity for both the exciton and the band-edge transition is used. The exciton binding energy of 170 meV leads to a reasonable transverse reduced band mass of $\mu_\perp = 0.15$. More experimental evidence as to the nature of the *GS*2, *GS*3 transition in GaS, however, has to be presented, before conclusive answers can be given. In particular, electroreflectance measurements as carried out on the 3.4-eV structure (*S*1) of GaSe should certainly be helpful in answering the question about the exis-

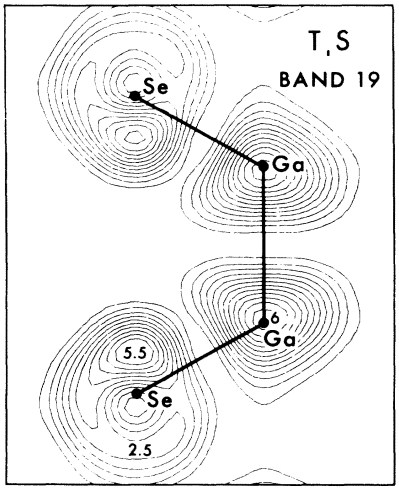

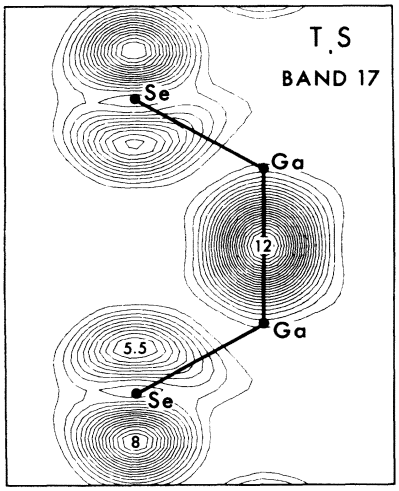

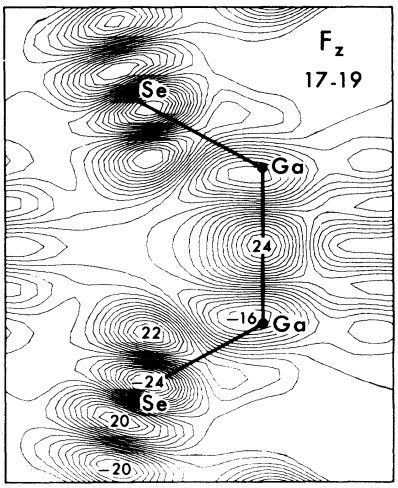

FIG. 10. Charge-density and transition function contour plots for one representative transition (*GS*2) of the group of transitions exhibiting intermediate ($\Delta \approx 400$ meV) energy shift in GaSe as displayed in Fig. 8. For explanations see caption of Fig. 7.

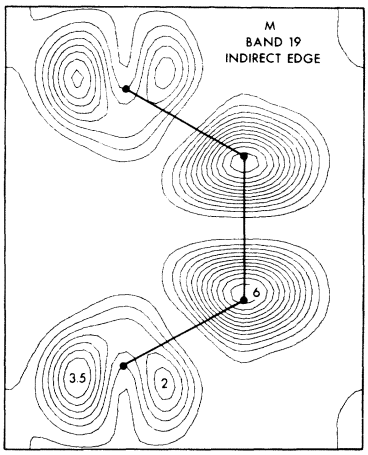

FIG. 11. Charge-density contour plot of the M_3^+ conduction-band minimum forming the indirect band edge in GaSe. Units are the same as in Fig. 7.

tence of excitonic character in the *GS*2 transition. However, our experiments along these lines on GaS were unsuccessful.

The intermediate energy shifts Δ for all GSn transitions are illustrated by the calculated charge-density contour maps for the *GS*2 transition in GaSe (Fig. 10). Both initial state (band 17 along *T*, *S*) and final state (band 19 along *T*, *S*) show charge distributions of mixed cation and anion character. The Ga–Ga bonding-antibonding charge distribution is basically involved in all transitions between the topmost valence-band pair and the lowest conduction-band pair (see also the transitions *G*1, *G*2 and the direct and indirect gaps). Its relative amount, however, depends on the exact location of the transition in $\vec{k}$ space (i.e., on the relative amount of anion-cation hybridization of the wave functions). While at the point *H* the anion admixture is very small (Fig. 7, transitions *G*1, *G*2), it increases along the lines *S* and *T* (Fig. 10, transition *GS*2) to reach maximum values at Γ (direct gap). The optical transition function F_z (for polarization $\vec{E} \parallel \vec{c}$), which is presented in Fig. 10 (bottom figure) illustrates the approximately equal contribution of anion and cation to the *GS*2 transition. According to Fig. 10 most of the energy shift Δ of the *GS*2 transition with anion substitution seems to originate from a valence-band shift. It is interesting to note that the indirect gap obviously belongs to the class of intermediate energy shift Δ.[6] Theoretically, this is also found by inspecting the charge-density contour map of the indirect conduction-band edge (band 19 at *M*), presented in Fig. 11 and the valence-band edge (band 18 at Γ), presented at the end of this section.

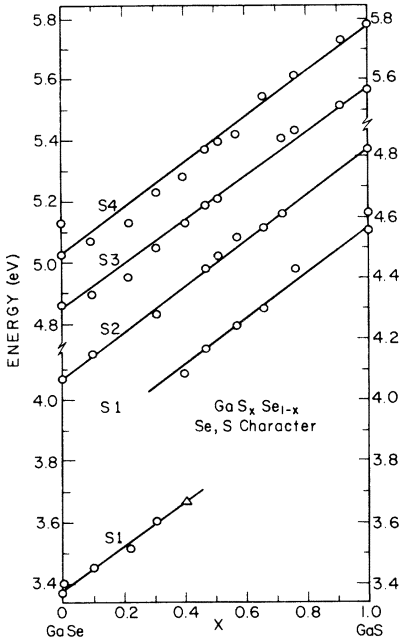

FIG. 12. Energy diagram of reflectivity structures, labeled *S*1 to *S*4 exhibiting strong ($\Delta \approx 780$ meV) energy shift. Labeling refers to predominant anion (Se, S) character of the involved wave functions.

Again, at M the conduction band contains relatively little anion character and the energy shift of the indirect gap transition is caused by the shift of the valence band at Γ which contains considerable Se p_z-like charge.

C. Transitions with predominant anion (S, Se) character and strong energy shifts ($\Delta = 780$ meV)

Four main transitions *S*1 to *S*4 which exhibit a large energy shift $\Delta \simeq 780$ meV are shown in Fig. 12. The high-energy doublet *S*3-*S*4 observed at 4.86 and 5.13 eV in GaSe can be followed through the series up to 5.57 and 5.78 eV, respectively, in GaS. The structure *S*2 is weakly seen in GaSe but it becomes important in GaS where it merges with the *GS*4 line. The low-energy structure *S*1 corresponds in GaSe to the anisotropic three-dimensional M_0 c.p. exciton which has been discussed at length in Sec. III. It shifts linearly to higher energy with increasing sulfur concentration and disappears at $x \approx 0.3$ and 0.4. No equivalent structure can be observed in GaS at the extrapolated energy range. The same difficulty has previously been reported in absorption measurements carried out at 90 °K.[42] Our modulation measurements, however, show a pronounced doublet at 4.55 and 4.61 eV in GaS, very similar to the *S*1 doublet observed at 5 °K in GaSe. The similarity of the line shapes is explicitly shown in Fig. 13. It is suggestive that these similar structures can be assigned to the same transition since they exhibit identical energy shifts and both disappear at a composition range of $x \approx 0.3$ and 0.4. The doublet splitting in GaS is about 60 meV, twice the splitting observed for GaSe. This difference can reasonably be explained by different exciton binding energies. The sudden changes in transition energies at $x \approx 0.3$ and 0.4 are presumably due to the structural transition from γ, ϵ to β-type stacking reported in this composition range.[6] This structural transition has also been found to be responsible for a 50-meV step in both direct- and indirect-gap energies[6] and for the intensity drop-off of the 135 cm^{-1} Raman mode[11] associated with the β polytype. In the case of the *S*1 transition the step is about 400 meV which would indicate a high sensitivity to stacking sequences of the states involved. Energy shifts owing to different polytypes have also been found in PbI_2 by Doni *et al.* by inspecting the reflectivity spectrum of the 2*H* and the 4*H* polytype.[48]

In Fig. 14 charge densities and the F_{xy} transition function for the *S*1 transition are displayed. As mentioned before, the final state, which is at Γ in the first conduction-band pair, has partially antibonding Ga-Ga character combined with strong Se *s*, p_z-type character. This explains the sensitivity of the Γ state (band 19) to anion substitution. Moreover, the initial state (band 16) exhibits exclusively Se p_{xy} character and therefore is also strongly affected. The corresponding transition is strongly localized on the anion site as shown in Fig. 14 (bottom picture) and corresponds mainly to an Se p_{xy} to *s* atomiclike transition.

The direct gap at Γ at ~2 eV also shows the strong experimental shift $\Delta \approx 780$ meV if selenium is substituted by sulfur.[6] In Fig. 15 the corresponding charge-density distributions and the transition function illustrate this behavior. The Γ state of the top valence band (band 18) has in addition to Ga-Ga bonding character, a strong, nearly pure Se p_z-like character. It is therefore

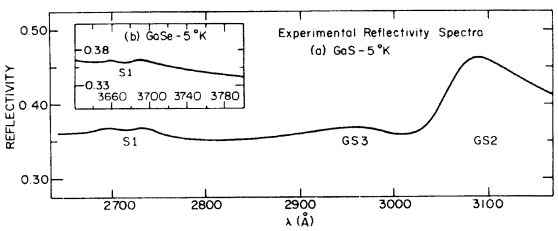

FIG. 13. Experimental reflectivity spectra (5 °K) of the double structure *S*1 in (a) GaSe around 3.4 eV and (b) GaS around 4.6 eV.

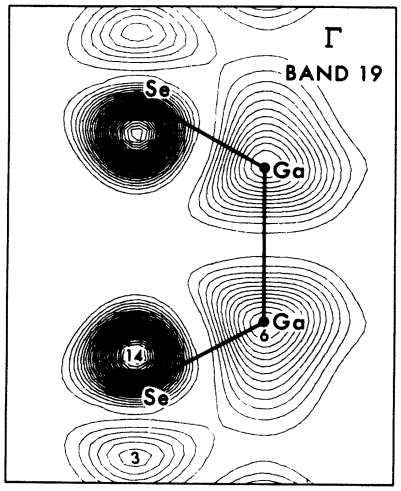

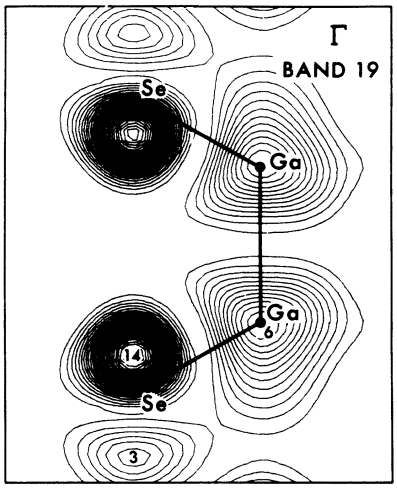

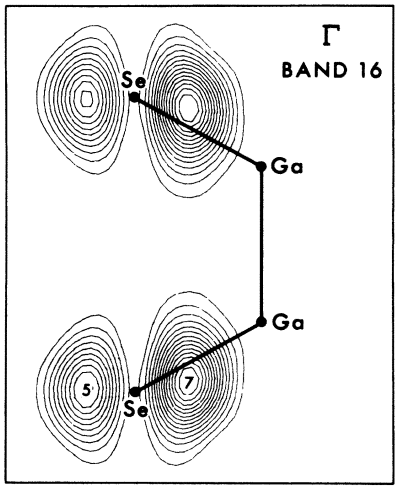

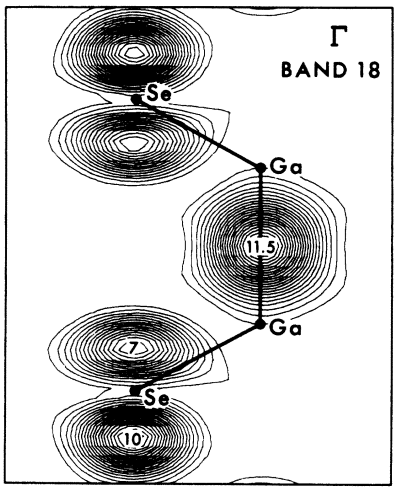

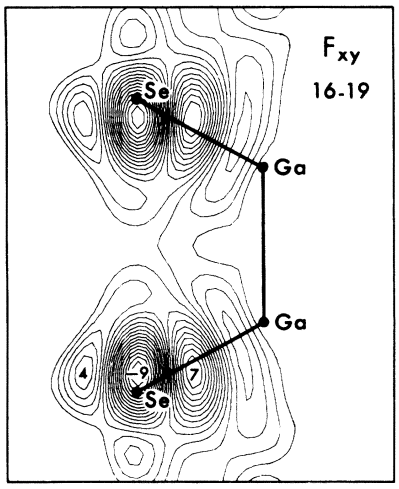

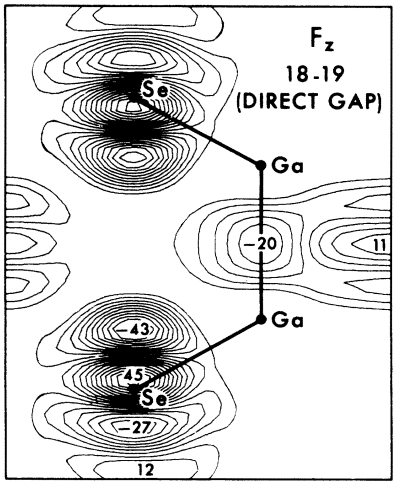

FIG. 14. Charge-density and transition function contour plots for one representative transition ($S1$) in GaSe of the group of transitions exhibiting strong ($\Delta \approx 780$ meV) energy shift as displayed in Fig. 12. For explanations see caption of Fig. 7.

FIG. 15. Charge-density and transition function contour plots for the direct-gap transition around 2.0 eV in GaSe. For explanations see caption of Fig. 7.

also sensitive to anion substitution. As was claimed earlier[8,17] the direct-gap transition corresponds partially to the excitation of the Ga–Ga bond. However, as seen from the transition function in Fig. 15, considerable contributions originate from anion p_z to s atomiclike transitions. This has not been emphasized before. It is clearly responsible for the large energy shift Δ of the direct gap.

In concluding this section, a simple argument which follows directly from the previous analysis can be given to explain the positive energy shifts Δ of optical transitions in the GaS_xSe_{1-x} mixed crystal series. The various charge-density contour maps reveal the varying amount of anion *nonbonding*, atomiclike charge contained in the various states. A direct qualitative relation between the amount of anion charge in initial and final states and the observed energy shift Δ can be established. In those cases in which the states contain contributions from anions, the transition mainly takes place between atomic p-like and s-like states. As compared to the selenium case, the atomic p (occupied) and s (unoccupied) states of sulfur show a wider energy separation (about 0.5 eV) which is directly reflected in an energy increase of the optical transitions in GaS_xSe_{1-x} with increasing x. Thus, the main result of our spectral analysis of the mixed-crystal series is that the gross changes in the optical spectra can be attributed directly to pure atomiclike behavior rather than to changes in ionicity or bond length.

V. CONCLUSIONS

New precise low-temperature reflectivity and wavelength modulated reflectivity measurements on Bridgeman-grown GaSe crystals are presented for energies ranging from 3 to 6 eV. In addition room-temperature electroreflectance measurements have been performed and used to identify the nature of particular transitions. A marked double structure in the reflectivity at 3.4 eV is interpreted as a three-dimensional anisotropic M_0 c.p. transition with excitonic character.

A new pseudopotential band structure is presented which affords a semiquantitative interpretation of the observed structures. The new band structure is a simple modification of a previous calculation (Ref. 8) in that the Ga-Ga atomic distance is increased to twice the covalent radius of gallium. With this slight modification a theoretical spectrum was obtained which exhibits all the marked features of the experimental spectrum. The main theoretical results consist of the identification of the observed prominent spectral structures in terms of $\vec{k}$ space location and atomiclike character of the transitions. A simplified picture of the optical response function of GaSe between 3 and 6 eV can thus be given. The low-energy peak at 3.8 eV originates from transitions between the uppermost valence-band pair and the first conduction-band pair around T and S in $\vec{k}$ space and corresponds to an excitation of the Ga–Ga bond combined with transitions between nonbonding selenium p_z and s states. The high-energy peak around 5.0 eV originates mainly from transitions starting from the lower-lying Ga-Se bands around Σ and also ending in the first conduction-band pair. These transitions occur exclusively between selenium p_{xy} and s states. These two groups of transitions, which roughly determine the lower part of the reflectivity spectrum of GaSe, to take place at locations in $\vec{k}$ space which are close to crystal-symmetry-determined "special $\vec{k}$ points." It therefore seems that the spectrum of GaSe can adequately be approximated by evaluating the band structure at two "special" $\vec{k}$ points. In addition to these overall features a rich fine structure can be resolved and identified in terms of the atomiclike character of the states involved in the transitions. On the basis of this knowledge the spectral changes occurring in a GaS_xSe_{1-x} mixed-crystal series are interpreted. Detailed experimental measurements are performed on the series for x ranging from 0 to 1 with steps of about 0.1. The experimental spectra between 3 and 6 eV (with the inclusion of direct and indirect gap at about 2 eV) can be decomposed into *three* main classes of transitions according to their energy shifts occurring with anion substitution. The three classes are characterized by zero ($\Delta = 0$), intermediate ($\Delta \approx 400$ meV), and strong ($\Delta \approx 780$ meV) energy shifts. A direct correspondence is found between the observed shifts and the calculated amount of atomiclike charge on the anion in GaSe. The relationships are illustrated by calculated charge-density contour maps and by real-space resolved contour maps of the transition functions $\vec{F}(\vec{r}) = \psi_i(\vec{r})\vec{p}\psi_f(\vec{r})$ which determine the optical dipole matrix elements $\vec{M}_{if} = \int F(\vec{r})\, d\vec{r}$. As a result the transition can similarly be grouped into three classes characterized by no or little charge ($\Delta \approx 0$), an intermediate amount of charge ($\Delta \approx 400$ meV), and a large amount of charge ($\Delta \approx 780$ meV) in initial and final states localized on the anions. With increasing anion charge the states are more sensitive to anion substitution resulting in increasing energy shifts Δ. This analysis connects the main changes in the optical spectra of GaS_xSe_{1-x} mixed crystals with differences in the atomic spectra of sulfur and selenium.

We acknowledge helpful collaboration in the growth of the crystals with the members of the Laboratoire de Physique Appliquée in Lausanne, Switzerland. Part of this work was done under the auspices of the U.S. ERDA.

*Present address: Bell Laboratories, Murray Hill, N. J. 07974.
†On leave from University of Montpellier and supported by a NATO fellowship.
‡Supported by a Swiss National Science Foundation Fellowship.
§Supported in part by the NSF Grant No. DMR72-03206-A02.

[1]K. Schubert, E. Dörre, and M. Kluge, Z. Metallk. 46, 216 (1955).
[2]F. Jellinek and H. Hahn, Z. Naturforsch. B 16, 713 (1961).
[3]Z. S. Basinski, D. B. Dove, and E. Mooser, Helv. Phys. Acta 34, 373 (1961).
[4]J. C. J. M. Terhell and R. M. A. Lieth, Phys. Status Solidi A 10, 529 (1972).
[5]J. L. Brebner, J. Phys. Chem. Solids 25, 1427 (1964).
[6]E. Aulich, J. L. Brebner, and E. Mooser, Phys. Status Solidi 31, 129 (1969).
[7]A. Bourdon, J. Phys. (Paris) 35, C3-261 (1964).
[8]M. Schlüter, Nuovo Cimento B 13, 313 (1973).
[9]G. Ottaviani, C. Canali, F. Nava, Ph. Schmid, E. Mooser, R. Minder, and I. Zschokke, Solid State Commun. 14, 933 (1974).
[10]M. Hayek, O. Brafman, and R. M. A. Lieth, Phys. Rev. B 8, 2772 (1973).
[11]A. Mercier and J. P. Voitchovsky, Solid State Commun. 14, 757 (1974).
[12]J. L. Brebner and G. Fischer, Can. J. Phys. 41, 561 (1963).
[13]J. L. Brebner, J. Phys. Chem. Solids 25, 1427 (1964).
[14]A. Mercier, E. Mooser, and J. P. Voitchovsky, Phys. Rev. B 12, 4307 (1975).
[15]A. Mercier and J. P. Voitchovsky (unpublished).
[16]R. R. L. Zucca, Ph.D. thesis (University of California, Berkeley, 1970) (unpublished).
[17]E. Mooser and M. Schlüter, Nuovo Cimento B 18, 164 (1973).
[18]F. Bassani, D. L. Greenaway, and G. Fischer, in *Proceedings of the Seventh International Conference on the Physics of Semiconductors*, edited by M. Hulin (Dunod, Paris, 1964).
[19]A. Baldereschi, K. Maschke, and M. Schlüter, Helv. Phys. Acta 47, 434 (1974).
[20]S. Kohn, Y. Petroff, and Y. R. Shen, Surf. Sci. 37, 205 (1973).
[21]R. Mamy, L. Martin, G. Leveque, and C. Raisin, Phys. Status Solidi B 62, 201 (1974); also see P. Thiry, R. Pincheaux, D. Dagneaux, and Y. Petroff, in *Proceedings of the Twelfth International Conference on the Physics of Semiconductors*, edited by M. H. Pilkuhn (Teubner, Stuttgart, 1974), p. 1324 and (unpublished).
[22]S. P. Kowalczyk, L. Ley, F. R. McFeely, and D. A. Shirley, Solid State Commun. 17, 463 (1975).
[23]C. Kittel in *Introduction to Solid State Physics*, 4th Ed. (Wiley, New York, 1971), p. 129.
[24]A. Baldereschi, Phys. Rev. B 7, 5212 (1973).
[25]D. J. Chadi and M. L. Cohen, Phys. Rev. B 7, 692 (1973).
[26]J. R. Chelikowsky and M. L. Cohen, Phys. Rev. Lett. 31, 1582 (1973).
[27]V. K. Subashiev, Le-Khac-Binh and L. S. Chertkova, Solid State Commun. 9, 369 (1971).
[28]V. I. Sokolov, D. B. Kushev, and V. K. Subashiev, Phys. Status Solidi B 50, K125 (1972).
[29]Y. Suzuki and Y. Hamakawa, J. Phys. Soc. Jpn. 37, 108 (1974).
[30]A. Balzarotti, M. Piacentini, E. Burattini, and P. Picozzi, J. Phys. C 4, L273 (1971).
[31]Y. Sasaki, C. Hamaguchi, and J. Nakai, J. Phys. C 5, L95 (1972).
[32]A. Balzarotti and M. Piacentini, Solid State Commun. 10, 421 (1972).
[33]Y. Sasaki, C. Hamaguchi, and J. Nakai, J. Phys. Soc. Jpn. 38, 162 (1975).
[34]For the minimum Γ_3^+ of the conduction band, the effective masses are determined from optical and electrical experiments (Ref. 9) to be $m_{c\parallel}=0.3$ and $m_{c\perp}=0.17$.
[35]R. J. Elliott, Phys. Rev. 108, 1384 (1957).
[36]M. Shinada and S. Sugano, J. Phys. Soc. Jpn. 21, 1936 (1966).
[37]E. O. Kane, Phys. Rev. 180, 852 (1963).
[38]A. Baldereschi and M. G. Diaz, Nuovo Cimento B 68, 217 (1970); J. A. Deverin, Helv. Phys. Acta 42, 397 (1969).
[39]P. C. Leung, G. Andermann, W. G. Spitzer, and C. A. Mead, J. Phys. Chem. Solids 27, 849 (1966).
[40]A rough parabolic fit results in $m_{\parallel}\approx 2-4\ m_0$ and $m_{\perp}\approx 1.5\ m_0$ for the 16th band at Γ.
[41]N. A. Gasanova, G. A. Akhundov, and M. A. Nizamet-Dinova, Phys. Status Solidi 17, K131 (1966).
[42]N. P. Gavaleshko, M. V. Kurik, A. S. Savtchuk, and G. B. Delevskii, Phys. Status Solidi B 65, K19 (1974).
[43]Ch. E. Moore, Atomic Energy Levels (National Bureau of Standards 467, 1952) (unpublished).
[44]J. A. Van Vechten and T. K. Bergstresser, Phys. Rev. B 1, 3351 (1970).
[45]D. Auvergne, J. Camassel, M. Mathieu, and A. Joullie, J. Phys. Chem. Solids 35, 133 (1974).
[46]M. Cordona, Solid State Phys. Suppl. S 11, (1969).
[47]B. Pistoulet, H. Mathieu, J. Camassel, and D. Auvergne, Phys. Status Solidi 39, 363 (1970).
[48]E. Doni, G. Grosso, G. Harbeke, E. Meier, and E. Tosatti, Phys. Status Solidi 68, 569 (1975).